Signal Interpretation for Monitoring and Diagnosis, A Cooling System Testbed

Eric-J. Manders, *Student Member, IEEE*, Gautam Biswas, *Member, IEEE*, Pieter J. Mosterman, Lee A. Barford, and Robert J. Barnett

***Abstract*—This paper discusses a method for fault detection and isolation in continuous dynamic systems. A key aspect of this approach is the coupling of a qualitative diagnosis engine and a monitoring system that computes symbolic feature values through a signal-to-symbol transformation on the continuously sampled measurement data. Signal analysis techniques with a sound statistical basis are employed to generate reliable symbolic data. The methodology is evaluated on the diagnosis of engineered faults in the cooling system of an automobile engine that has been instrumented with temperature and pressure sensors. Results show the interdependency between modeling for diagnosis and the feature extraction system.**

***Index Terms*—Fault diagnosis, feature extraction, instrumentation, monitoring, symbolic signal analysis, transient analysis.**

I. Introduction

Diagnosis of faults in engineering systems is the process of detecting anomalous system behavior and isolating its cause. This paper adopts a *model-based* approach to fault detection and isolation (FDI) of continuous dynamic systems based on *analytical redundancy* techniques. The fault isolation algorithms apply qualitative constraint analysis methods that effectively realize a *parameter estimation* scheme. Model parameters correspond directly to system components and estimated parameter values that deviate from their expected values implicate the associated components. The qualitative approach avoids difficulties in the convergence, precision, and computational complexity of established numerical parameter estimation methods, especially when system behavior is nonlinear. Because qualitative methods process input in symbolic form, a *signal interpretation* step is required to compute symbolic feature values from continuously sampled data using *signal-to-symbol* transformation techniques.

The current work focuses on the diagnosis of *abrupt* faults that correspond to instantaneous and persistent parameter value changes. Abrupt faults result in transient behavior of system variables, and transient analysis becomes critical for accurate fault isolation [1]. It follows then that the symbolic representation of the observations must capture the transient dynamics.

Fig. 1 shows the architecture of TRANSCEND, a comprehensive model-based approach to diagnosis [1]. Vector u is the input to the physical process under diagnostic scrutiny, and vector y is the set of observations made on the system. An observer model (a set of differential equations) generates the expected system behavior $\hat{y}$ and an observer tracks the residuals $r = y - \hat{y}$ to correct for small deviations in the estimated state vector $\hat{x}$ using a standard gain matrix scheme [3]. The residuals are also input to the symbol generation unit that computes the symbols for the diagnosis modules.

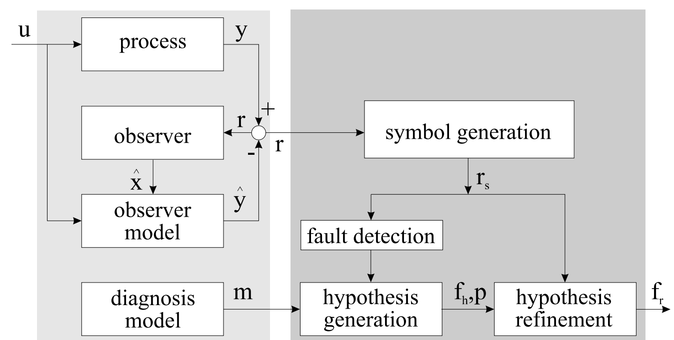

Fig. 1. TRANSCEND architecture.

The diagnosis model incorporates the dependency relations between component parameters and the observed variables in the form of a *temporal causal graph* (TCG), a directed graph structure that captures algebraic and temporal constraints between system variables [1], [2]. Fault detection triggers a fault isolation scheme that consists of *hypothesis generation* and *hypothesis refinement*. Hypothesis generation uses the diagnosis model, m, and the symbolic residuals, r_s, to generate a set of hypothesized fault candidates, f_h, from observed deviations, and to predict behavior, p, for each fault candidate. During hypothesis refinement spurious candidates are eliminated from the set by matching new observations against the predictions predictions to arrive at the final diagnosis result, f_r.

The modeling methodology and diagnosis algorithms of TRANSCEND have been described in other work [1], [2]. In this paper, the monitoring component is described in the context of experiments with a real testbed. Section II describes the signal-to-symbol transformation methods used. Section III describes a testbed constructed around the cooling system of an automobile

Manuscript received May 26, 1999; revised February 10, 2000.

This work was supported in part by a grant from the Hewlett-Packard Corporation.

Eric Manders and Gautam Biswas are with the Department of Electrical Engineering and Computer Science, Vanderbilt University, P.O. Box 1824 Station B, Nashville, Tennessee 37235. Phone: +1 615 322-2771, fax: +1 615 343-6702. Email: {manders,biswas}@vuse.vanderbilt.edu

Pieter Mosterman is with the Institute of Robotics and Mechatronics, DLR Oberpfaffenhofen, P.O. Box 1116, D-82230 Wessling, Germany. Email: Pieter.J.Mosterman@dlr.de

Lee Barford is with Agilent Laboratories, 1501 Page Mill Road, MS 4AD, Palo Alto, California 94303-0889. Email: lee_barford@labs.agilent.com

Joel Barnett is with the Department of Mechanical Engineering, Vanderbilt University. Email: joelbar@vuse.vanderbilt.edu

Publisher Item Identifier S 0018–9456(00)04539-3.

internal combustion engine. Section IV presents experimental results, and section V presents a summary and conclusions of this work.

II. Signal-to-Symbol Transformation

In the design of the signal-to-symbol transformation, the set of symbols is determined by the hypothesis generation and refinement algorithms. The challenge is to design or select algorithms that compute these symbols from actual measurement data.

A. Symbolic description of transient behaviors

Fault detection is the task of identifying deviating measurements while monitoring system behavior. A deviating measurement triggers the hypothesis generation process that takes as input qualitative magnitude deviation values: *normal*, *high*, and *low*, represented by the symbols "0", "$+$" and "$-$" respectively. The hypothesis generation algorithm then identifies a set of possible fault candidates and for each candidate computes a fault *signature* for all measured variables. The signature is the prediction of signal behavior immediately after the point of failure and is a tuple of magnitude and first and higher order derivative values expressed as "0", "$+$" and "$-$" symbols. Conflicting qualitative influences may lead to an unknown prediction for a variable, indicated by the symbol "$\cdot$".

During hypothesis refinement the signatures are matched against the symbolic signal features. In the present implementation these symbolic features include the qualitative magnitude and slope values, where slope values are computed only after an initial magnitude deviation has been detected. Higher order features are not computed, but TRANSCEND's *progressive monitoring* mechanism exploits higher order derivative values in the signature based on the notion that as time progresses, higher order derivatives will increasingly contribute to the description of the signal behavior [1]. Hypothesis refinement is further enhanced if discontinuous changes in the signals can be detected. An additional symbol, "$\star$", indicates an abrupt magnitude change in the signal.

The computation of the symbols listed above constitute the signal-to-symbol transformation algorithms. The symbolic values are assigned based on signal statistics but do not have an uncertainty factor or probabilistic attribute. The specific algorithms are discussed next.

B. Magnitude changes and discontinuities

Detecting a change in a signal implies the use of a decision function to determine whether the signal is deviating from its normal behavior or not. The decision function uses a threshold that provides a design trade-off between sensitivity to changes and the rate of false alarms of the detector. The threshold value is typically based on the *signal-to-noise ratio* of the signal, and the performance of the detector can be analyzed if the noise model is known. In general it is not desirable to attenuate the noise with a linear filter because that also smoothes nonlinear transient dynamics such as discontinuities.

Because a threshold crossing does not preserve information on the nature of the change, the labeling of discontinuous changes must occur in parallel. The detection of discontinuous changes has been studied from the viewpoint of local frequency analysis as well as statistical hypothesis testing [4]. The experiments in this paper employ the hypothesis testing approach, where the signal is represented as a random process with a known probability distribution. An abrupt change is modeled as a change in a parameter value of the probability distribution. The signal is an independent random variable sequence y_k with probability density function $p_\theta(y_k)$, where θ is the signal model parameter that is being monitored for change. The abrupt change detection problem can be formulated as a multiple hypothesis testing problem. The change hypothesis, H_1, is tested against the default hypothesis, H_0 [6]:

$$\begin{cases} H_0 : \theta = \theta_0 \\ H_1 : \theta = \theta_1, \end{cases}$$

where θ_0 and θ_1 represent the parameter value before and after the change, respectively. The central quantity in constructing the test statistic is the *log-likelihood ratio*, $s(y) = \ln \frac{p_{\theta_1}(y)}{p_{\theta_0}(y)}$. The cumulative log-likelihood ratio, $S_j^k = \sum_{i=j}^{k} s_i$, (where $s_i = \ln \frac{p_{\theta_1}(y_i)}{p_{\theta_0}(y_i)}$ and j, k define a discrete time window) shows a negative drift before a change in θ, and a positive drift afterwards. This property is the basis for the CUSUM algorithm with decision function S_j^k. In diagnosis problem solving θ_0 is known, but the magnitude of the parameter change, and thus θ_1, is not known. For this case the decision function is modified to use the maximum likelihood estimate of θ_1, and the resulting algorithm is the *Generalized Likelihood Ratio* (GLR) ([6]):

$$g_k = \max_{1 \le j \le k} \sup_{\theta_1} S_j^k.$$

The stopping rule is given by $t_a = \min\{k : g_k \ge h\}$, where t_a is the *detection time* and h is a predefined threshold.

Fig. 2 shows the GLR applied to a signal with additive noise. A lower signal-to-noise ratio implies a longer delay in change detection. A closed form expression for the decision function for this change detection problem can be found in [4].

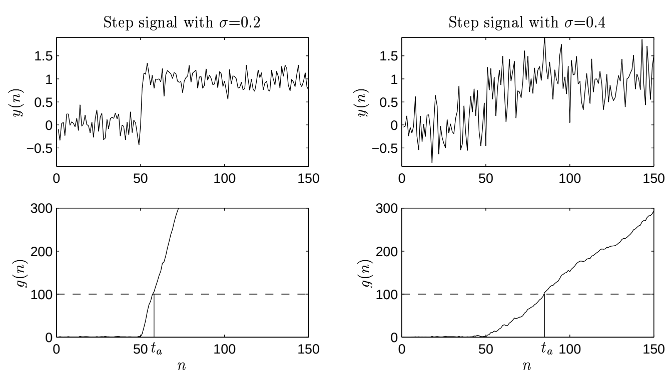

Fig. 2. Detection of a step change in a signal with a GLR detector, for two levels of additive Gaussian noise. The change point is at n = 50.

C. Slope estimation

To design a slope estimator consider first the ideal discrete-time differentiator with frequency response $H(e^{j\omega}) = j\omega$, for

$|\omega| \leq \pi$. The filter that exhibits this response is noncausal and has infinite length, and any practical slope estimator will be an approximation of the ideal differentiator. The first-order difference operator, $y'(n) = y(n) - y(n-1)$, is an example of a straightforward approximation. This operator has frequency response $H(e^{j\omega}) = 1 - cos\,\omega + j\,sin\,\omega$, which approximates the ideal response for low frequencies ($\omega \ll \pi$), but deviates significantly from the ideal filter when ω approaches π (e.g., [7]). The accuracy of the estimator is improved by increasing the sampling rate. However, the main problem with the difference operator is the sensitivity to noise, a consequence of the strict high-pass characteristic. For diagnosis, robust feature extraction is crucial, and low sensitivity to noise is an important design goal of the estimator. The solution taken here is to use a linear finite impulse response filter that minimizes the noise power gain in the derivative signal [8]. The coefficients for an unbiased minimum variance derivative estimate filter are found as the solution of a linearly constrained least squares problem [9]. A filter with more coefficients will have a more robust derivative estimate. Higher order derivative estimation filters can be found in a similar way by modeling the signal as a piecewise polynomial with the same degree as the order of the desired derivative.

Fig. 3 illustrates derivative estimation with the filter and the first-order difference operator for a signal without and with noise.

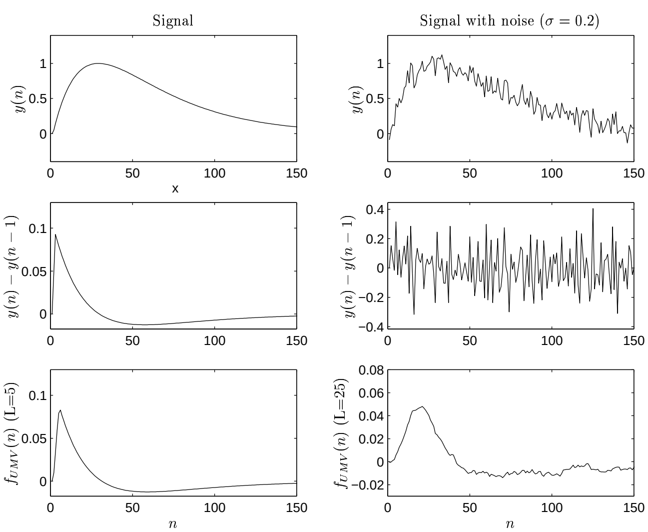

Fig. 3. Comparison of derivative estimation with a first-order difference operator, and an unbiased minimum variance derivative estimate filter (f_{UMV}).

III. EXPERIMENT DESIGN AND TESTBED IMPLEMENTATION

A. Selection of the device under test

Evaluating TRANSCEND on a real system requires a *device under test* that exhibits complex dynamic behaviors and provides challenges similar to those that might be encountered in a complex industrial system. Knowledge about the system should be sufficient so that a well defined dynamic model can be constructed. Practical considerations also demand that sensors introduced in the system will not affect its operation and that faults introduced in a controlled experiment will not permanently damage the device. Based on these considerations and the available expertise and parts, an automobile internal combustion engine, specifically a Chevrolet V-8, was selected as the device under test.

The diagnosis experiments discussed in this paper relate to the engine cooling system. In an automotive cooling system a liquid coolant is pumped through a pressurized closed loop to remove heat from the engine block and dissipate it through the radiator. A schematic of such a cooling system is shown in Fig. 4. Fault detection and isolation in this system presents a combined mechanical, thermal, and fluid flow problem, and the diagnosis model captures mechanical, thermodynamic, and hydraulic aspects of the cooling system operation. The model includes the lower and upper hose, the radiator, the thermostat and the pump as components that may fail, possibly in more than one way. Each component has multiple model parameters associated with it. The cooling system operation and the diagnosis model are described in detail in [4]. A number of faults can be introduced into the cooling system without damaging the engine, provided the temperature of the engine block does not exceed certain limits. Examples are: thermostat failure (open or closed), broken hose or failed hose connection, radiator leak, pump or fan belt failure, and clogged radiator.

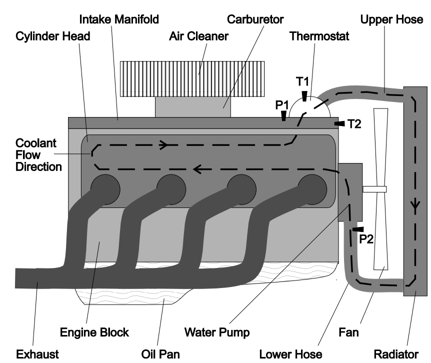

Fig. 4. Engine schematic with sensor placement (T1, T2, P1, P2).

B. Experimental Setup

The testbed is made up of the engine, bolted to a frame and connected to an exhaust system, and an instrumentation system that consists of a personal computer equipped with an internal data acquisition board (Data Translation, DT3001-PGL), and data acquisition software (Data Translation). A custom built external enclosure provides connectors for the sensors and holds a screw terminal interface to the data acquisition board. All sensor leads are shielded to reduce electrical interference from the ignition system. The coolant temperature and pressure are measured at several places in the cooling system circuit (see Fig. 4) and chosen by our expert for ease of sensor installation and discriminating ability.

Two temperature sensors have been installed, one in the thermostat housing downstream from the thermostat (T1), and a second in the intake manifold, just upstream from the thermostat (T2). T2 is close to the cylinder heads where the coolant temperature is highest. The sensors are rugged transition joint probe type thermocouples with ungrounded junction and stainless steel sheath (Omega TJ-36CXSS-18U). Cold junction compensation circuitry for the thermocouples is built onto the screw terminal. The response time for this thermocouple configuration, with both sensors immersed in coolant fluid, is in the order of a few seconds, which is sufficient to capture the thermal transients.

Two pressure sensors have been installed, one in the intake manifold next to the thermostat housing (P1), providing a pressure measurement immediately downstream of the thermostat, and a second in the lower radiator hose immediately after the radiator outlet (P2). The sensors are amplified voltage output transducers, suitable for harsh environments, and measure absolute pressure up to 345 kPa (Omega PX176-050A5V). The measurement bandwidth is 50 Hz, sufficient to capture the near instantaneous pressure changes due to large leaks in the system. Operable temperature range is up to 125 $^\circ$C with a temperature compensated range up to 85 $^\circ$C.

During the experiments the engine is operated in steady state and without load. It is assumed that faults are introduced after the cooling system has reached a known steady state. Under this condition the steady state values become the nominal values. Fault isolation is currently performed off-line on collected data. The sample time, 0.02 s, was established empirically. Symbolic feature values are computed every second, thus subsampling the actual sensor data. A median filter of length 5 is applied to all signals to remove outliers.

IV. Results

The methodology described above is illustrated with two experiments. In each experiment a different type of coolant leak fault is introduced by draining coolant from the system through a valve. The model parameter associated with a leak fault is a resistance, 'R_{leak}'. The lower hose of the cooling system is fitted with a T-junction coupling to which a valve can be attached. A large leak, which mimics a hose puncture or a failed hose connection, is created by using a high outflow lever operated gate valve that can be opened and closed very fast. A small leak is created by using a ball valve that can be controlled more precisely. A small leak in the lower hose is very similar to a leak in the bottom of the radiator itself.

Fig. 5 shows the result of the large leak scenario. When the valve is opened, coolant drains from the system very quickly. The valve is closed again after a few seconds so that some coolant remains in the system and overheating of the engine is avoided. The transients that result from closing the valve are ignored. Fig. 5(a) shows a graph of the measurement data during the transient. The rapid decrease in pressure and a slower increase in temperature can clearly be seen. The level of physical detail in the model is such that a large leak corresponds to a discontinuous pressure decrease, and thus should be captured accordingly. Fig. 5(b) shows the output of the signal to symbol transformation algorithms for the TRANSCEND diagnosis steps. The steps to which these symbols correspond are indicated as time points in the graphs of Fig. 5(a) also. The rate at which the symbols are computed corresponds to the model, i.e., the signal-to-symbol transformation is designed to detect a discontinuous change within one TRANSCEND step. Step 0 is defined as the time at which the initial deviation is detected and hypotheses generation is triggered. An abrupt change is detected in each pressure signal during step 0 also. At step 1, slope detection is triggered for the pressure signals and hypotheses refinement is initiated which completes at step 2. Monitoring of a signal is suspended when specific transient characteristics have been detected, e.g. the signal is moving towards steady state, or certain second order phenomena have been detected. The stopping conditions are evaluated on a per signal basis. In this example monitoring is suspended earlier because of the dynamics that result from closing the valve. Fig. 5(c) shows the fault isolation results. The table shows the symbolic values for the measurement data at step 2 and the fault signatures of the remaining fault candidates. Fault signatures for this example include up to the second order derivatives. The diagnosis is accurate because it includes the actual fault $R_{leak}-$. The negative sign indicates a decrease in the leak resistance, in effect, a decrease from an infinitely high value when the valve is closed, to a finite value when the valve is opened. Fault isolation also generated one spurious candidate: $I_{rad-out}+$, an increase in the radiator outflow inertia, that cannot be distinguished from the true fault with this set of observations. The complete hypothesis refinement process for this fault is described in [4].

Fig. 6 depicts the results for a small leak. No discontinuous change is detected at the point of failure, and the temperature measurements do not change significantly.[1] The monitoring system is tuned so that a "0" slope symbol is generated for an absolute slope value < 0.05 . With a derivative filter of length 25 the derivative signal still takes quite long to converge to this value since the derivative reaches 0 asymptotically. A simple heuristic that requires consecutive derivative values to fall within the threshold interval increases the sensitivity, and the "0" slope symbol is first computed at step 15. The fault isolation results are less specific for this fault, additional discriminating information from the discontinuous behavior is lacking.

V. Conclusions

The development of a suitable testbed is vital to demonstrate the utility of research results in monitoring and diagnosis of complex dynamic systems. The study of qualitative analysis methods that require symbolic feature values computed from real data, and their comparison with predictions generated by the model lead to new insights on model building and the use of signal analysis algorithms. Sophisticated signal-to-symbol transformation methods are critical to compute robust feature values.

The experiments illustrate the interdependency of modeling and instrumentation of a system under diagnostic scrutiny. A parameter change that results in transients with dynamic effects exceeding the measurement bandwidth of the system, should correspond to a structural change in the model. A model switching approach will be incorporated into the diagnosis system by considering hybrid modeling techniques that are being developed in other work [10]. Analysis of the model will then provide information on the appropriate signal-to-symbol transformation algorithms that should be applied to the signals, e.g.,

[1] The system is in fact still moving towards steady state asymptotically, hence the barely noticeable slope in the temperature data.

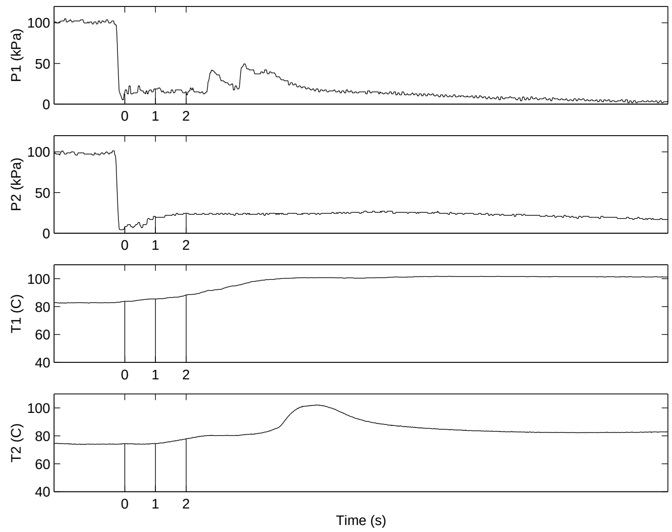

(a) Data segment

Step	T1	T2	P1	P2
0	$(0,\cdot)$	$(0,\cdot)$	$(-,\cdot,\star)$	$(-,\cdot,\star)$
1	$(+,\cdot)$	$(0,\cdot)$	$(-,-)$	$(-,+)$
2	$(+,+)$	$(+,\cdot)$	$(-,-)$	$(-,0)$

(b) Signal-to-Symbol Transformation

step 2

	actual	
	P1:	$-\ -$
	P2:	$-\ 0$
	T1:	$+\ +$
	T2:	$+\ +$
$R_{leak}-$	P1:	$-\ \cdot\ \cdot$
	P2:	$-\ \cdot\ \cdot$
	T1:	$0\ +\ \cdot$
	T2:	$0\ +\ \cdot$
$I_{rad-out}+$	P1:	$-\ \cdot\ \cdot$
	P2:	$-\ \cdot\ \cdot$
	T1:	$0\ \cdot\ \cdot$
	T2:	$0\ \cdot\ \cdot$

(c) Final diagnosis result, $R_{leak}-$ is the actual fault.

Fig. 5. Fault detection and isolation for a large leak in the lower hose.

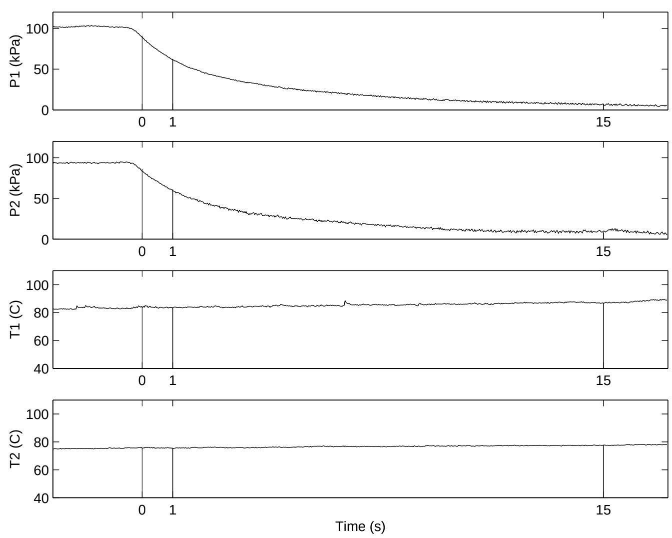

(a) Data segment

Step	T1	T2	P1	P2
0	$(0,\cdot)$	$(0,\cdot)$	$(-,\cdot)$	$(-,\cdot)$
1	$(0,\cdot)$	$(0,\cdot)$	$(-,-)$	$(-,-)$
15	$(0,\cdot)$	$(0,\cdot)$	$(-,0)$	$(-,0)$

(b) Signal-to-Symbol Transformation

Step 15

	actual	
	P1:	$-\ -$
	P2:	$-\ -$
	T1:	$0\ \cdot$
	T2:	$0\ \cdot$
$R_{rad-out}+$	P1:	$-\ -\ -$
	P2:	$-\ -\ -$
	T1:	$0\ 0\ \cdot$
	T2:	$0\ 0\ 0$
$I_{rad-out}+$	P1:	$-\ -\ +$
	P2:	$-\ -\ +$
	T1:	$0\ \cdot\ \cdot$
	T2:	$0\ 0\ -$
$C_{rair}+$	P1:	$-\ -\ -$
	P2:	$-\ -\ -$
	T1:	$0\ 0\ \cdot$
	T2:	$0\ 0\ +$
$R_{leak}-$	P1:	$-\ -\ +$
	P2:	$-\ -\ +$
	T1:	$0\ +\ -$
	T2:	$0\ 0\ -$

(c) Final diagnosis result, $R_{leak}-$ is the actual fault.

Fig. 6. Fault detection and isolation for a small leak in the lower hose.

abrupt change detection should only be applied to those signals where discontinuous changes can occur in the model.

TRANSCEND also allows for a systematic analysis of sensor placement, based on evaluating the diagnosability of the model. This analysis will be performed on the cooling system in future work.

ACKNOWLEDGMENTS

The authors acknowledge the help of Philippus Feenstra with experiments and modeling of the cooling system.

REFERENCES

[1] P. J. Mosterman and G. Biswas, "Diagnosis of continuous valued systems in transient operating regions," *IEEE Trans. on Systems, Man and Cybernetics*, vol. 29, no. 6, pp. 554–565, 1999.

[2] P. J. Mosterman and G. Biswas, "Monitoring, prediction, and fault isolation in dynamic physical systems," in *AAAI-97*, Rhode Island, Aug. 1997, pp. 100–105.

[3] K. Brammer and G. Siffling, *Kalman-Bucy Filters*, Artec House, Norwood MA, 1989.

[4] E. J. Manders, P. J. Mosterman, and G. Biswas, "Signal to symbol transformation techniques for robust diagnosis in TRANSCEND," in *Tenth International Workshop on Principles of Diagnosis*, Loch Awe, Scotland, 1999, pp. 155–165.

[5] P. J. Mosterman, G. Biswas, and E. J. Manders, "A comprehensive framework for model based diagnosis," in *Ninth International Workshop on Principles of Diagnosis*, Cape Cod, MA, USA, May 1998, pp. 86–94.

[6] M. Basseville and I.V. Nikiforov, *Detection of abrupt changes: theory and applications*, Prentice-Hall, 1993.

[7] M. J. Chantler, S. Daus, T. Vikatos, and G. M. Coghill, “The use of quantitative dynamic models and dependency recording for diagnosis,” in *Seventh International Workshop on Principles of Diagnosis*, Val Morin, Canada, Oct. 1996, pp. 59–68.

[8] O. Vainio, M. Renfors, and T. Saramaki, “Recursive implementation of FIR differentiators with optimum noise attenuation,” *IEEE Trans. on Instrumentation and Measurement*, vol. 46, no. 5, pp. 1202–1207, Oct. 1997.

[9] L. Barford, E. J. Manders, G. Biswas, P. J. Mosterman, V. V. Ram, and J. Barnett, “Derivative estimation for diagnosis,” in *Workshop on Emergent Technologies (EMTECH99)*, pp. 9–12. IEEE, Venice, Italy, 1999.

[10] P. J. Mosterman, G. Biswas, and J. Sztipanovits, “A Hybrid Modeling and Verification Paradigm for Embedded Control Systems,” *Control Engineering Practice: An IFAC Journal*, vol. 6, pp. 511–521, Apr. 1998.

Eric-Jan Manders (S’91) is a Ph.D. candidate in the Department of Electrical Engineering and Computer Science at Vanderbilt University. He received his ’Ingenieur’ (Ir.) degree, equivalent to the M.S., in Electrical Engineering from Delft University of Technology, The Netherlands, in 1991. His research interests include signal processing, pattern recognition, instrumentation, fault detection and isolation, and embedded systems. He is conducting his graduate research in the area of the coupling of numerical and symbolic methods for signal analysis and interpretation with applications to diagnosis problem solving.

Gautam Biswas is an Associate Professor of Computer Science and Engineering, and Management of Technology at Vanderbilt University. He received a B.Tech. degree in Electrical Engineering from the Indian Institute of Technology, Bombay, India, in 1977, and M.S. and Ph.D. degrees in Computer Science from Michigan State University, East Lansing, in 1979 and 1983, respectively. Dr. Biswas conducts research in Artificial Intelligence with primary interests in modeling and analysis of complex systems and their applications to diagnosis, design, and control. His research is currently supported by NSF, ONR, PNC Japan, and Hewlett-Packard Laboratories. He has published in a number of journals and contributed book chapters. Dr. Biswas has served on the Program Committee of a number of conferences and was co-chair of the 1996 Workshop on Principles of Diagnosis, and on the Senior Program committee for AAAI-97 and AAAI-98. He is a Senior member of the IEEE Computer Society, ACM, AAAI, and the Sigma Xi Research Society.

Pieter J. Mosterman is a research associate at the Control Design Engineering group of the Institute of Robotics and Mechatronics at the German Aerospace Center (DLR), Oberpfaffenhofen. He received a B.Sc. and M.Sc. from the University of Twente, The Netherlands, in 1987 and 1991, respectively. In 1997 he received a Ph.D. in Electrical and Computer Engineering from Vanderbilt University, Nashville, Tennessee. Currently, he is investigating the requirements for modeling complex dynamic systems, which involves integrating sophisticated formalisms for modeling and simulating both continuous time and discrete event phenomena. He has published in a number of journals and contributed book chapters.

Lee A. Barford is a Senior Scientist and Project Manager with Agilent Laboratories, Palo Alto, California. He received a B.A. in Mathematics and Computer Science from Temple University in 1982, and an M.Sc. and Ph.D. in Computer Science from Cornell University in 1985 and 1987 respectively. At Agilent, Dr. Barford leads research in image processing, dynamical systems theory, statistics, and distributed systems as applied to current industrial problems in industrial inspection, monitoring and diagnosis, and data-driven identification of complex nonlinear systems ranging from manufacturing processes to microwave circuits.

Robert Joel Barnett is a senior Research Associate in Mechanical Engineering at Vanderbilt University. He received a B.Sc., M.Sc., and Ph.D. in Mechanical Engineering from Vanderbilt University in 1970, 1978 and 1993, respectively. Dr. Barnett’s research interests include automotive systems diagnosis, and real-time analysis of weld pool dynamics and weld pool solidification mechanics. Prior to his affiliation with Vanderbilt University, he served as President of Mid-South Engineering, Inc., and was involved in research collaboration with NASA and DARPA projects. He has published in the area of welding sensing, modeling, and control. He is a member of the Society of Automotive Engineers, and Pi Tau Sigma Honor Society.